References

1 Hanahan D, Weinberg RA. The hallmarks of cancer. *Cell* 2000; **100**: 57–70.
2 Hahn WC, Weinberg RA. Modelling the molecular circuitry of cancer. *Nat Rev Cancer* 2002; **2**: 331–41.
3 Calabretta B, Perrotti D. The biology of CML blast crisis. *Blood* 2004; **103**: 4010–22.
4 Mullighan CG, Goorha S, Radtke I *et al.* Genome-wide analysis of genetic alterations in acute lymphoblastic leukaemia. *Nature* 2007; **446**: 758–64.
5 Mullighan CG, Miller CB, Radtke I *et al.* BCR-ABL1 lymphoblastic leukaemia is characterized by the deletion of Ikaros. *Nature* 2008; **453**: 110–4.
6 Clarke MF, Dick JE, Dirks PB *et al.* Cancer stem cells – perspectives on current status and future directions: AACR Workshop on cancer stem cells. *Cancer Res* 2006; **66**: 9339–44.
7 Wakabayashi Y, Inoue J, Takahashi Y *et al.* Homozygous deletions and point mutations of the Rit1/Bcl11b gene in γ-ray induced mouse thymic lymphomas. *Biochem Biophys Res Commun* 2003; **301**: 598–603.
8 Kominami R, Niwa O. Radiation carcinogenesis in mouse thymic lymphomas. *Cancer Sci* 2006; **97**: 575–81.
9 Kaminura K, Mishim O, Ohi H *et al.* Haploinsufficiency of Bcl11b for suppression of lymphomagenesis and thymocyte development. *Biochem Biophys Res Commun* 2007; **355**: 538–42.
10 Nagel S, Kaufmann M, Drexler HG, MacLeod RA. The cardiac homeobox gene NKX2-5 is deregulated by juxtaposition with BCL11B in pediatric T-ALL cell lines via a novel t(5;14)(q35.1;q32.2). *Cancer Res* 2003; **63**: 5329–34.
11 MacLeod RA, Nagel S, Kaufmann M, Janssen JW, Drexler HG. Activation of HOX11L2 by juxtaposition with 3'-BCL11B in an acute lymphoblastic leukemia cell line (HPB-ALL) with t(5;14)(q35;q32.2). *Genes Chromosomes Cancer* 2003; **37**: 84–91.
12 Przybylski GK, Dik WA, Wanzeck J *et al.* Disruption of the BCL11B gene through inv(14)(q11.2q32.31) results in the expression of BCL11B-TRDC fusion transcripts and is associated with the absence of wild-type BCL11B transcripts in T-ALL. *Leukemia* 2005; **19**: 201–8.
13 Wakabayashi Y, Watanabe H, Inoue J *et al.* Bcl11b is required for differentiation and survival of αβT lymphocytes. *Nat Immunol* 2003; **4**: 533–9.
14 Inoue J, Kanefuji T, Okazuka K, Watanabe H, Mishima Y, Kominami R. Expression of TCRβ partly rescues developmental arrest and apoptosis of αβT cells in Bcl11b-/- mice. *J Immunol* 2006; **176**: 5871–9.
15 Arlotta P, Molyneaux BJ, Chen J, Inoue J, Kominami R, Macklis JD. Neuronal subtype-specific genes that control corticospinal motor neuron development in vivo. *Neuron* 2005; **45**: 207–21.
16 Golonzhka O, Liang X, Messaddeq N *et al.* Dual role of COUP-TF-interacting protein 2 in epidermal homeostasis and permeability barrier formation. *J Invest Dermatol* 2008; **129**: 1459–70.
17 Golonzhka O, Metzger D, Bornert JM *et al.* Ctip2/Bcl11b controls ameloblast formation during mammalian odontogenesis. *Proc Natl Acad Sci USA* 2009; **106**: 4278–83.
18 Avurum Albu DI, Feng D, Bhattacharya D *et al.* BCL11B is required for positive selection and survival of double-positive thymocytes. *J Exp Med* 2007; **204**: 3003–15.
19 Okazuka K, Wakabayashi Y, Kashihara M *et al.* p53 prevents maturation of T cell development to the immature CD4-CD8+ stage in Bcl11b-/- mice. *Biochem Biophys Res Commun* 2005; **328**: 545–9.
20 Fischer A, Malissen B. Natural and engineered disorders of lymphocyte development. *Science* 1998; **280**: 237–43.
21 Gounari F, Aifantis I, Khazaie K *et al.* Somatic activation of beta-catenin bypasses pre-TCR signaling and TCR selection in thymocyte development. *Nat Immunol* 2001; **2**: 863–9.
22 Xu Y, Banerjee D, Huelsken J, Birchmeier W, Sen JM. Deletion of beta-catenin impairs T cell development.Nat Immunol. *Nat Immunol* 2003; **4**: 1177–82.
23 Staal FJ, Clevers HC. Wnt signaling in the thymus. *Curr Opin Immunol* 2003; **15**: 204–8.
24 Ohi H, Mishima Y, Kamimura K, Maruyama M, Sasai K, Kominami R. Multi-step lymphomagenesis deduced from DNA changes in thymic lymphomas and atrophic thymuses at various times after γ-irradiation. *Oncogene* 2007; **26**: 5280–9.
25 Yamamoto T, Morita S, Go R *et al.* Clonally expanding thymocytes having lineage capability in g-ray induced mouse strophic thymus. *Int J Radiat Oncol Biol Phys* (in press).
26 Xu M, Sharma A, Wiest DL, Sen JM. Pre-TCR-induced β-catenin facilitates transversal through β-selection. *J Immunol* 2009; **182**: 751–8.
27 Xu M, Sharma A, Hossain MZ, Wiest DL, Sen JM. Sustained expression of pre-TCR induced beta-catenin in post-beta-selection thymocytes blocks T cell development. *J Immunol* 2009; **182**: 759–65.
28 Weerkamp F, Baert MR, Naber BA *et al.* Wnt signaling in the thymus is regulated by differential expression of intracellular signaling molecules. *Proc Natl Acad Sci USA* 2006; **103**: 3322–6.
29 Carleton M, Haks MC, Smeele SA *et al.* Early growth response transcription factors are required for development of $CD4^-CD8^-$ thymocytes to the $CD4^+CD8^+$ stage. *J Immunol* 2002; **168**: 1649–58.
30 Xi H, Kersh GJ. Early growth response gene 3 regulates thymocyte proliferation during the transition from $CD4^-CD8^-$ to $CD4^+CD8^+$. *J Immunol* 2004; **172**: 964–71.
31 Aifantis I, Gounari F, Scorrano L, Borowski C, von Boehmer H. Constitutive pre-TCR signaling promotes differentiation through Ca^{2+} mobilization and activation of NF-kappaB and NFAT. *Nat Immunol* 2001; **2**: 403–9.
32 Engel I, Murre C. E2A proteins enforce a proliferation checkpoint in developing thymocytes. *EMBO J* 2004; **23**: 202–11.
33 Gregorieff A, Clevers H. Wnt signaling in the intestinal epithelium: from endoderm to cancer. *Genes Dev* 2005; **19**: 877–90.
34 Guo Z, Dose M, Kovalovsky D *et al.* Beta-catenin stabilization stalls the transition from double-positive to single-positive stage and predisposes thymocytes to malignant transformation. *Blood* 2007; **109**: 5463–72.
35 Ioannidis V, Beermann F, Clevers H, Held W. The β-catenin-TCF-1 pathway ensures $CD4^+CD8^+$ thymocyte survival. *Nat Immunol* 2001; **2**: 691–7.
36 Mullighan CG, Phillips LA, Su X *et al.* Genomic analysis of the clonal origins of relapsed acute lymphoblastic leukemia. *Science* 2008; **322**: 1377–80.

18. O. Golonzhka *et al.*, *J. Invest. Dermatol.* **129**, 1459 (2009).
19. See supporting material on *Science* Online.
20. R. S. Welner *et al.*, *Blood* **109**, 4825 (2007).
21. C. A. Vosshenrich *et al.*, *J. Exp. Med.* **204**, 2569 (2007).
22. W. Dontje *et al.*, *Blood* **107**, 2446 (2006).
23. H. Shigematsu *et al.*, *Immunity* **21**, 43 (2004).
24. C. H. Martin *et al.*, *Nat. Immunol.* **4**, 866 (2003).
25. H. Takatori *et al.*, *J. Exp. Med.* **206**, 35 (2009).
26. C. A. Vosshenrich *et al.*, *Nat. Immunol.* **7**, 1217 (2006).
27. D. M. Gascoyne *et al.*, *Nat. Immunol.* **10**, 1118 (2009).
28. S. Doulatov *et al.*, *Genes Dev.* **23**, 2076 (2009).
29. A. P. Weng *et al.*, *Genes Dev.* **20**, 2096 (2006).
30. M. Ciofani, J. C. Zúñiga-Pflücker, *Immunol. Res.* **34**, 117 (2006).
31. M. Ciofani, G. C. Knowles, D. L. Wiest, H. von Boehmer, J. C. Zúñiga-Pflücker, *Immunity* **25**, 105 (2006).
32. G. Bain, W. J. Romanow, K. Albers, W. L. Havran, C. Murre, *J. Exp. Med.* **189**, 289 (1999).
33. T. Kreslavsky *et al.*, *Proc. Natl. Acad. Sci. U.S.A.* **106**, 12453 (2009).
34. We thank P. Liu, H. Kawamoto, P. Li, T. Ikawa, D. Scripture-Adams, and members of the Rothenberg lab for sharing unpublished results and helpful discussion; D. Metzger and J.-M. Bornert for help with generation of the floxed Bcl11b mice; H.-Y. Kueh for guidance in data analysis; T. Taghon and F. Costantini for vectors and mice; D. Perez and R. Diamond for flow cytometry support; and R. Butler and S. Washburn for animal care and breeding supervision. Supported by a California Institute for Regenerative Medicine fellowship (L.L.), NIH grants R33 HL089123 and RC2 CA148278 (E.V.R.), NIH grant R01 GM60852 (M.L.), the Caltech–City of Hope Biomedical Initiative, the Louis Garfinkle Memorial Laboratory Fund, the Al Sherman Foundation, and the A. B. Ruddock Professorship.

Supporting Online Material

www.sciencemag.org/cgi/content/full/329/5987/89/DC1
Materials and Methods
SOM Text
Figs. S1 to S11
Tables S1 and S2
References

2 March 2010; accepted 19 May 2010
10.1126/science.1188989

An Essential Developmental Checkpoint for Production of the T Cell Lineage

Tomokatsu Ikawa,[1] Satoshi Hirose,[2] Kyoko Masuda,[1] Kiyokazu Kakugawa,[1] Rumi Satoh,[1] Asako Shibano-Satoh,[1] Ryo Kominami,[2] Yoshimoto Katsura,[1,3] Hiroshi Kawamoto[1]*

In early T cell development, progenitors retaining the potential to generate myeloid and natural killer lineages are eventually determined to a specific T cell lineage. The molecular mechanisms that drive this determination step remain unclarified. We show that, when murine hematopoietic progenitors were cultured on immobilized Notch ligand DLL4 protein in the presence of a cocktail of cytokines including interleukin-7, progenitors developing toward T cells were arrested and the arrested cells entered a self-renewal cycle, maintaining non-T lineage potentials. Reduced concentrations of interleukin-7 promoted T cell lineage determination. A similar arrest and self-renewal of progenitors were observed in thymocytes of mice deficient in the transcription factor Bcl11b. Our study thus identifies the earliest checkpoint during T cell development and shows that it is Bcl11b-dependent.

T cells are generated from multipotent hematopoietic stem cells through a series of differentiation steps. The first step in this pathway is the generation of progenitors that have lost erythroid/megakaryocyte potential but retain the capacity to generate other hemopoietic cells, including myeloid, T, and B cells (*1*–*6*). We and others have recently identified the next stage, in which the T cell progenitors have lost B cell potential but are still able to generate myeloid cells, dendritic cells (DCs), and natural killer (NK) cells (*7*, *8*). Therefore, the most critical step for development of the T cell lineage is now thought to be at the point where myeloid potential is terminated.

We sought to identify the step at which progenitors become fully committed to the T cell lineage and what regulates this transition. A reliable way to substantiate that a given step is critical for the development of a lineage is to demonstrate developmental arrest at the stage before that step under particular conditions. In the case of B cell differentiation, deletion of *E2a*, *Ebf*, or *Pax5* genes leads to an early developmental arrest before formation of a functional *IgH* chain gene; these arrested B cell progenitors undergo self-renewal and remain B lineage uncommitted, with the potential to develop along other lineages, including myeloid and T cell (*9*–*11*). This case illustrates that such a critical developmental checkpoint exists at the step when uncommitted B cell progenitors become determined to the B cell lineage. Unlike the B cell lineage, to date no such checkpoint has been identified for the T cell lineage before the initiation of *TCR* gene rearrangement.

As T cell progenitors develop, they proceed through developmental stages referred to as DN1 to DN4 (double-negative $CD4^-CD8^-$) that can be tracked by surface phenotype. The DN2 stage can be subdivided into two stages based on transgenic green fluorescent protein (GFP) expression controlled by the proximal lck (plck) promoter (lck is a src family kinase selectively expressed by T cells). GFP^- cells retain non-T lineage potential, including that for myeloid cells, DCs, and NK cells, whereas the latter stage GFP^+ cells are determined to the T cell lineage (*7*, *12*). We designate these two stages DN2mt (myeloid-T) and DN2t (T-lineage determined) and term the step between these stages the DN2-determination step. This determination step is thought to be the first critical checkpoint in T cell development (*13*).

We cultured lineage-negative (Lin^-) $c\text{-}kit^+$ $Sca\text{-}1^+$ (LKS) cells from 13 days post-coitum (dpc) murine fetal liver with immobilized Delta-like 4 (DLL4) protein in the presence of the cytokines SCF (stem cell factor), Flt3L (FMS-like tyrosine kinase ligand), and interleukin (IL)–7 (fig. S1). After 7 days of culture, cells remained at the DN stage (Fig. 1A, left panel), whereas in the control group, where cells were cultured with TSt-4 stromal cells expressing DLL4 (TSt-4/DLL4), generation of $CD4^+CD8^+$ double-positive (DP) cells was observed (fig. S2). Upon closer analysis on DN cells generated in the feeder-free condition, we observed that these cells resembled DN2mt cells (maintained $c\text{-}kit^{high}CD25^+$) (Fig. 1A, right panel) and thus named them FFDN2 cells (feeder-free-cultured DN2-like cells). By several criteria, the FFDN2 cells appeared identical to DN2mt cells: (i) they gave rise to authentic αβ T cells when transferred to a TSt-4/DLL4 stromal coculture system (fig. S3, A and B); (ii) they retained the potential to produce macrophages (Fig. 1B), NK cells, and DCs (fig. S3, C and D); (iii) intracellular T cell receptor (TCR) β chain protein was not expressed (Fig. 1C); and (iv) their gene expression profiles were similar to those of DN2mt cells (Fig. 1D and fig. S4). Furthermore, GFP expression was not observed in FFDN2 cells generated from progenitors isolated from plck-GFP mice (Fig. 1E). It is unlikely that this arrest is due to the failure of TCR gene rearrangement because enforced expression of a functional TCRβ chain gene did not prevent the developmental arrest (fig. S5). FFDN2 cells could not generate B cells (fig. S3E), indicating that dedifferentiation to more primitive progenitors did not occur in this culture system. Of note, FFDN2 cells showed an almost unlimited in vitro expansion (Fig. 1F), while essentially maintaining c-kit and CD25 expression (Fig. 1G) and a developmental potential comparable to that of freshly isolated DN2mt cells (fig. S6). Cells in the $c\text{-}kit^+CD25^+$ fraction possessed the potential to maintain long-term culture, because long-term culture could be maintained by using $c\text{-}kit^+CD25^+$ cells at the time of passage (fig. S7). Such self-renewal capacity, together with our other results,

[1]Laboratory for Lymphocyte Development, RIKEN Research Center for Allergy and Immunology, Yokohama 230-0045, Japan. [2]Department of Molecular Genetics, Graduate School of Medical and Dental Sciences, Niigata University, Niigata 951-8510, Japan. [3]Division of Cell Regeneration and Transplantation, Advanced Medical Research Center, Nihon University School of Medicine, Tokyo 173-8610, Japan.

*To whom correspondence should be addressed. E-mail: kawamoto@rcai.riken.jp

indicated that the DN2-determination step may be a critical checkpoint for T cell development.

To investigate the molecular mechanisms of T cell lineage determination, we searched for an environmental cue that could drive the arrested cells through the DN2-determination step. After testing various cytokines and Notch ligand conditions in the feeder-free culture system, we found that FFDN2 cells initiate differentiation when the concentration of IL-7 is reduced on day 7 of culture (10 ng/ml to 1 ng/ml). In this induction system, GFP^+ DN3 cells appear on day 3 after IL-7 reduction (Fig. 2A). These cells did not express myeloid-lineage transcription factors *PU.1* (*Sfpi1*) and *C/EBPα*, whereas T cell lineage–associated genes such as *lck*, *Tcf1*, *pTα*, and *Bcl11b* were markedly up-regulated (Fig. 2B). Notably, cells in these cultures developed up to the αβTCR-

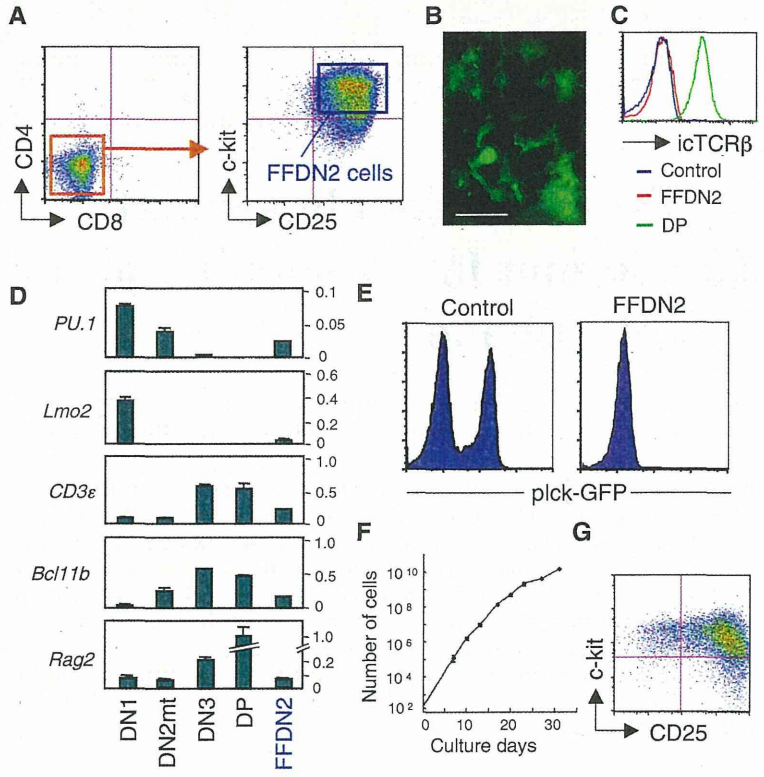

Fig. 1. Immobilized DLL4 with a combination of cytokines induces self-renewing expansion of immature thymocytes. **(A)** LKS progenitor cells (200 cells) from 13 dpc murine fetal liver were cultured with immobilized Fc-DLL4 supplemented with 10 ng/ml of SCF, IL-7, and Flt3L for 7 days. Generated cells were harvested and stained with the indicated antibodies and analyzed by a flow cytometry. Data are representative of four independent experiments. **(B)** A photomicrograph of macrophages generated from FFDN2 cells. FFDN2 cells induced from green mouse progenitors in a similar manner as (A) were sorted and cultured with TSt-4 stromal cells for 14 days in the presence of 10 ng/ml M-CSF (macrophage colony-stimulating factor). Macrophages are seen as large GFP^+ cells. Scale bar, 100 μm. **(C)** Expression of intracellular (ic) TCRβ in FFDN2 cells, in negative control cells generated in feeder-free culture using only the Fc portion (Control), and in positive control $CD4^+CD8^+$ DP cells from an adult thymus. **(D)** mRNA expression of lineage-specific genes in cells derived from DN1, DN2mt, DN3, DP, and FFDN2 cells determined by quantitative reverse transcription polymerase chain reaction (RT-PCR). Expression was normalized to acidic ribosomal protein (ARP) mRNA expression, and the mean + SD of triplicate samples is shown. Data are representative of three independent experiments. **(E)** Flow cytometric analysis of GFP expression in FFDN2 cells generated from progenitors of plck-GFP mice in comparison with cells generated under TSt-4/DLL4 conditions (Control). Data are representative of three independent experiments. **(F)** A growth curve of FFDN2 cells. Viable cells were enumerated at the indicated time points. **(G)** c-kit versus CD25 expression by FFDN2 cells after long-term culture. Fetal liver LKS cells were cultured under feeder (–) conditions for 30 days and then analyzed by flow cytometry. Data are representative of four independent experiments.

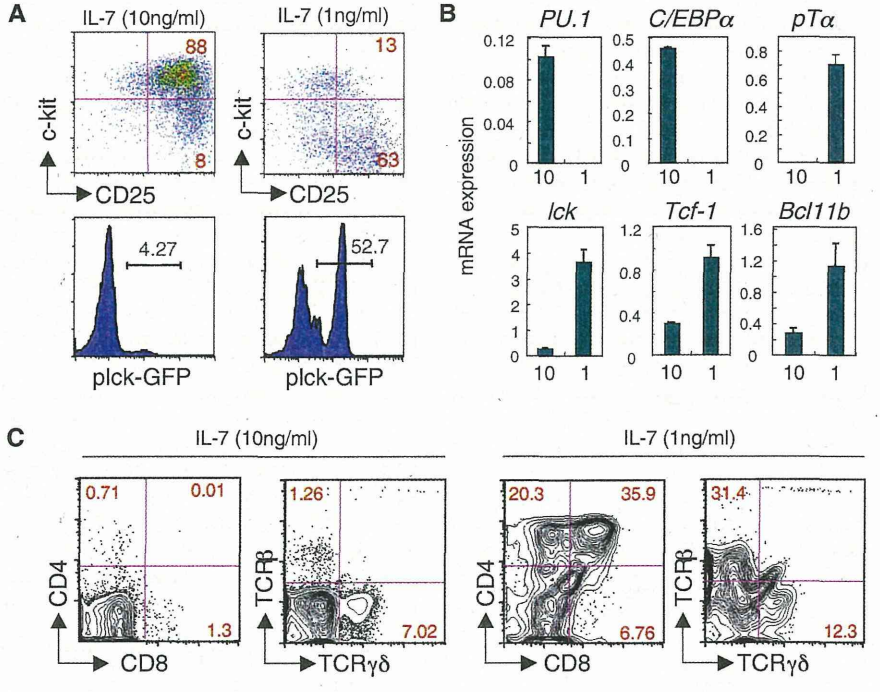

Fig. 2. Reduction of IL-7 concentration induces the generation of DP cells in feeder-free culture. **(A)** LKS cells (200 cells) from 13 dpc fetal liver were cultured with immobilized Fc-DLL4 in the presence of SCF, IL-7, and Flt3L (10 ng/ml). After 7 days, the concentration of IL-7 was maintained or reduced to 1 ng/ml, and the cells were cultured for an additional 3 days. Cells were analyzed by flow cytometry. Data are representative of three independent experiments. **(B)** mRNA expression of lineage-associated genes in cells cultured in the presence of 10 ng/ml or 1 ng/ml of IL-7 in the same manner as (A). Expression was normalized to ARP mRNA expression, and the mean + SD of triplicate samples is shown. Data are representative of three independent experiments. **(C)** Flow cytometric analysis of cells generated 7 days after switching to cultures with either high or low IL-7 concentration. Cells were analyzed for the expression of CD4 versus CD8 and TCRβ versus TCRγδ. Data are representative of five independent experiments.

expressing $CD4^+CD8^+$ DP stage (Fig. 2C and figs. S8 and S9). Although the kinetics of DP cell growth was delayed compared with that in the TSt-4/DLL4 feeder cell culture system, the final yield of DP cells was nearly identical (fig. S10). The DP cells generated by reducing the concentration of IL-7 appeared to be authentic DP cells, because they give rise to CD4 and CD8 single-positive (SP) cells when transferred to a fetal thymus organ culture system (fig. S11). These results demonstrated that $\alpha\beta TCR^+$ cells can be generated from prethymic progenitors in a "feeder-free" culture system and that the TCRβ-selection, which is thought to serve as the critical checkpoint for preTCR formation in progenitors, does not require additional environmental factors in this feeder-free culture system.

Often transcription factors regulate cell lineage determination steps. Among genes up-regulated by our induction system, we focused on *Bcl11b*, a T cell lineage–specific transcription factor originally identified as a tumor suppressor in murine T cell lymphoma (*14*). Bcl11b-deficient mice exhibit impaired thymocyte development around the DN3 to immature SP stage because of an inability to rearrange the V_β to D_β gene segments (*15*). We carefully reexamined the phenotype of fetal thymus cells from Bcl11b-deficient mice and found that, at 18 dpc, there was a developmental arrest at the DN2 stage (Fig. 3A). Despite this, the absolute number of DN2 cells was not increased (Fig. 3B), indicating that self-renewing expansion is not so prominent in vivo, a difference that could be due to the limited niche space in the thymus for early progenitors. We cultured these DN2 cells under TSt-4/DLL4 conditions, which can support T cell differentiation up to the DP stage. In such cultures, *Bcl11b*$^{-/-}$ cells continued to proliferate even after 4 weeks, maintaining their DN2 surface phenotype (Fig. 3C). Similar to FFDN2 cells, *Bcl11b*$^{-/-}$ DN2 cells exhibited features of DN2mt cells, including the potential to develop into macrophages and NK cells (Fig. 3D), and loss of B cell potential (fig. S12).

Bcl11b deficiency is lethal around the neonatal period (*15*). To investigate whether the developmental arrest of *Bcl11b*$^{-/-}$ progenitors is seen in the adult thymus, where T cells are continuously generated, we produced chimeric mice by transferring *Bcl11b*$^{-/-}$ fetal liver cells into irradiated B6Ly5.1 congenic mice. At 8 weeks after transfer, we observed nearly complete developmental arrest at the DN2 stage, with only a few DP cells (Fig. 3E). Similar to ex vivo fetal thymocytes of *Bcl11b*$^{-/-}$ mice and cultured *Bcl11b*$^{-/-}$ DN2 cells, the arrested DN2 cells were equivalent to DN2mt cells. There was no increase in thymic B cells in the recipients of the *Bcl11b*$^{-/-}$ fetal liver cells (fig. S13), indicating that the *Bcl11b*$^{-/-}$ DN2 cells that developed in the thymus did not dedifferentiate into more primitive progenitors in vivo.

The similar stage of arrest in the DLL4/IL-7 cultures and in the *Bcl11b*$^{-/-}$ mice suggested that the arrest in the cultures may be due to a failure to up-regulate Bcl11b. To examine this possibility, we retrovirally transduced Bcl11b cDNA into fetal liver LKS cells and cultured these transduced cells under DLL4/IL-7 conditions. The Bcl11b-transduced cells could give rise to DN3 cells even in the presence of a high concentration of IL-7 (Fig. 4A), and TCRβ gene rearrangement was enhanced (Fig. 4B), whereas myeloid-lineage–associated genes were suppressed (Fig. 4C), demonstrating that Bcl11b expression eliminated the DN2 arrest that occurred in the DLL4/IL-7 cultures.

As has been reported (*16*), the absence of Bcl11b had a severe impact on the generation of thymic αβT cells, whereas there was little effect on the generation of γδ T cells (fig. S14A). The same is true for cells generated in the DLL4/IL-7 cultures (fig. S14B). These results suggested that the segregation to the γδT cell lineage occurs before the DN2mt stage, although the possibility

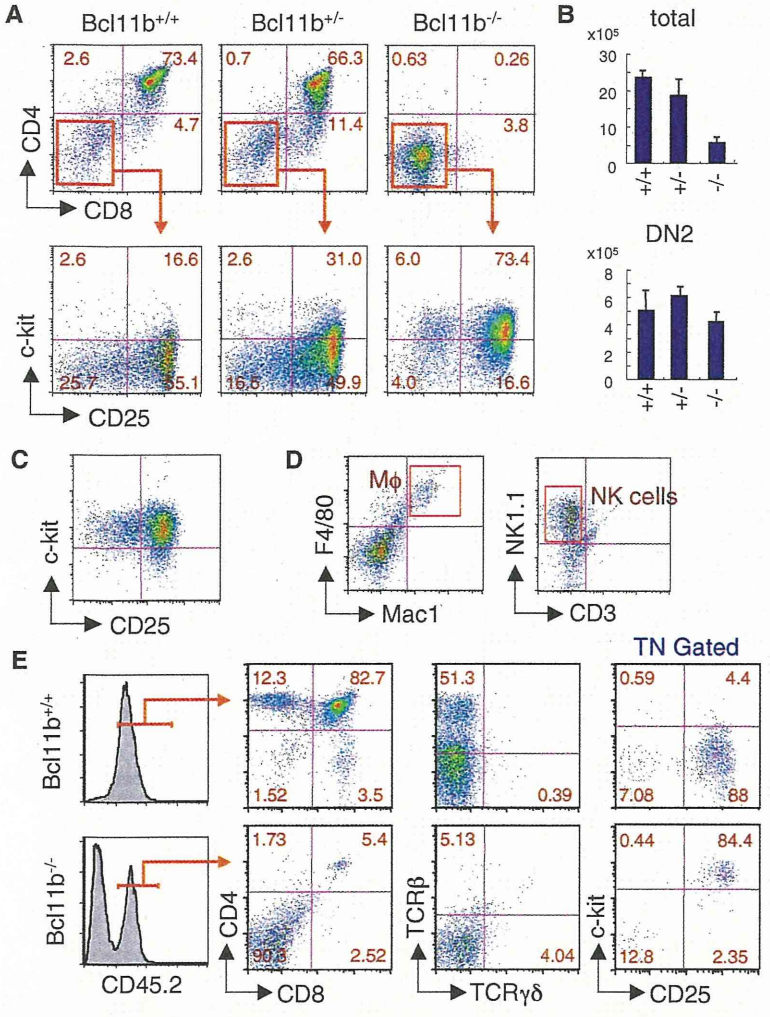

Fig. 3. Bcl11b is essential for T cell lineage determination. **(A)** Flow cytometric analysis of fetal thymocytes from *Bcl11b*$^{-/-}$ mice. Profiles are shown for CD4 versus CD8 of 18 dpc fetal thymocytes, and c-kit versus CD25 of cells gated in upper panels, from the indicated mice. For each group, more than five mice were individually analyzed, and representative profiles are shown. **(B)** Absolute numbers of total thymocytes and DN2 cells in 18 dpc fetuses of the indicated *Bcl11b* genotypes. More than five mice were individually analyzed for each group, and the mean + SD is shown. **(C)** Flow cytometric analysis of c-kit versus CD25 of fetal liver LKS cells from Bcl11b$^{-/-}$ mice cultured on TSt-4/DLL4 stromal cells for 30 days. Data are representative of three independent experiments. **(D)** Generation of macrophages and NK cells from cultured Bcl11b$^{-/-}$ fetal liver cells. The c-kit$^+$ CD25$^+$ cells shown in (C) were cultured (200 cells per well) for 7 days with TSt-4 cells in the presence of M-CSF (left panel) or IL-15 (right panel) and analyzed for macrophage and NK cell markers by flow cytometry. Data are representative of three independent experiments. **(E)** Fetal liver cells from Bcl11b$^{+/+}$ or Bcl11b$^{-/-}$ mice (Ly5.2) were transferred into lethally irradiated mice (Ly5.1). Flow cytometric profiles of reconstituted thymocytes of recipient mice 8 weeks after transfer are shown. In right panels, profiles of cells gated on CD3$^-$CD4$^-$CD8$^-$ [triple negative (TN)] fraction are shown. For each group, more than five mice were individually analyzed, and representative data are shown.

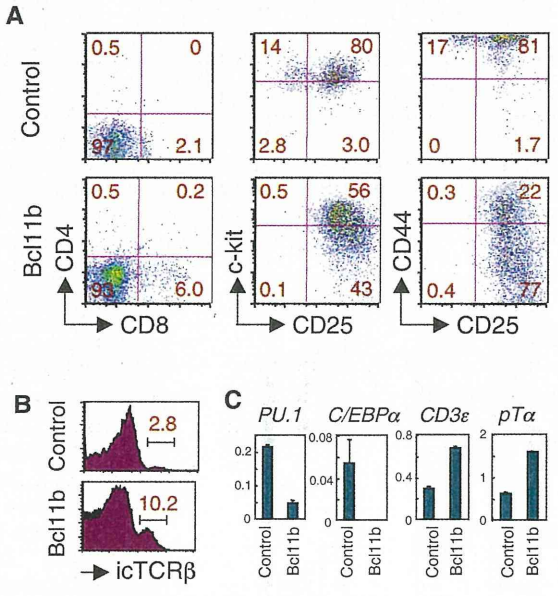

Fig. 4. Enforced expression of Bcl11b abrogated the DN2 arrest in the DLL4/IL-7 cultures. (**A** to **C**) LKS cells from 13 dpc B6 fetal liver were transduced with murine stem cell virus (MSCV)–Bcl11b or MSCV-control vector. Two days later, GFP$^+$ cells were sorted and cultured with immobilized Fc-DLL4 in the presence of 10 ng/ml of SCF, IL-7, and Flt3L for 7 days. Flow cytometric profiles of CD4 versus CD8, c-kit versus CD25, and CD44 versus CD25 expression (A), icTCRβ expression (B), and mRNA expression (C) in generated cells are shown. Expression of mRNA was normalized to ARP mRNA expression, and the mean + SD of triplicate samples is shown. Data are representative of three independent experiments.

still remains that the γδ T cells that had been generated from "leaky" DN3 cells underwent compensatory proliferation.

The developmental steps just after the formation of preTCR (DN3 stage) and αβ TCR (DP stage) serve as critical checkpoints (*16*, *17*), and cells that fail to pass these points succumb to apoptotic cell death. In contrast, the arrested progenitors at the DN2-determination step enter a self-renewal cycle. The appearance of self-renewing progenitors among *Bcl11b*$^{-/-}$ thymocytes may explain the previous findings that loss-of-function mutations in the *Bcl11b* gene are frequently observed in murine T cell lymphomas induced by γ irradiation (*14*) and that chromosomal aberration disrupting *Bcl11b* gene was identified in human T cell acute lymphoblastic leukemia cases (*18*), because the acquisition of self-renewal capacity is regarded as the first step in leukemia development. In this context, a similar outcome was recently observed when *Lmo2*, a known oncogene, was overexpressed in thymocytes and caused the cells to enter a self-renewal cycle in vivo (*19*).

The present study thus defines a Bcl11b-driven checkpoint at which T cell progenitors terminate non-T-lineage potential in order to become determined to the T cell lineage (fig. S15). Our finding that Bcl11b up-regulation can be triggered by an extrinsic cue, diminished IL-7, suggests that progression through the DN2-determination step is instructed by environmental signals in the thymus. It is quite likely that the reduction in IL-7 signaling is a physiological mediator of this step, because the IL-7R is dramatically down-regulated at the transition from the DN2 to the DN3 stage (*20*). Considering that Bcl11b is thought to be a transcriptional repressor, we speculate that Bcl11b directly suppresses myeloid-lineage–associated genes, such as *PU.1* or *C/EBPα*, and that such suppression is critical for differentiation toward the T cell fate.

A recent study demonstrated that Bcl11b is expressed in the T cell–like lymphoid cells of lamprey (*21*). Because a Bcl11b homolog has not been found in animals other than vertebrates (fig. S16), we propose that Bcl11b arose in phylogeny to construct a new lineage distinct from the preexisting innate type killer cells.

References and Notes

1. Y. Katsura, H. Kawamoto, *Int. Rev. Immunol.* **20**, 1 (2001).
2. M. Lu, H. Kawamoto, Y. Katsube, T. Ikawa, Y. Katsura, *J. Immunol.* **169**, 3519 (2002).
3. Y. Katsura, *Nat. Rev. Immunol.* **2**, 127 (2002).
4. J. Adolfsson *et al.*, *Cell* **121**, 295 (2005).
5. C. V. Laiosa, M. Stadtfeld, T. Graf, *Annu. Rev. Immunol.* **24**, 705 (2006).
6. H. Kawamoto, Y. Katsura, *Trends Immunol.* **30**, 193 (2009).
7. H. Wada *et al.*, *Nature* **452**, 768 (2008).
8. J. J. Bell, A. Bhandoola, *Nature* **452**, 764 (2008).
9. S. L. Nutt, B. Heavey, A. G. Rolink, M. Busslinger, *Nature* **401**, 556 (1999).
10. T. Ikawa, H. Kawamoto, L. Y. Wright, C. Murre, *Immunity* **20**, 349 (2004).
11. J. M. Pongubala *et al.*, *Nat. Immunol.* **9**, 203 (2008).
12. K. Masuda *et al.*, *J. Immunol.* **179**, 3699 (2007).
13. E. V. Rothenberg, J. E. Moore, M. A. Yui, *Nat. Rev. Immunol.* **8**, 9 (2008).
14. Y. Wakabayashi *et al.*, *Biochem. Biophys. Res. Commun.* **301**, 598 (2003).
15. Y. Wakabayashi *et al.*, *Nat. Immunol.* **4**, 533 (2003).
16. H. J. Fehling, H. von Boehmer, *Curr. Opin. Immunol.* **9**, 263 (1997).
17. Y. Takahama, *Nat. Rev. Immunol.* **6**, 127 (2006).
18. G. K. Przybylski *et al.*, *Leukemia* **19**, 201 (2005).
19. M. P. McCormack *et al.*, *Science* **327**, 879 (2010).
20. Q. Yu, B. Erman, J. H. Park, L. Feigenbaum, A. Singer, *J. Exp. Med.* **200**, 797 (2004).
21. P. Guo *et al.*, *Nature* **459**, 796 (2009).

22. The authors are grateful to C. Murre, T. Kadesch, Y. Agata, and S. Yamasaki for providing us with reagents and protocols, and to P. Burrows for critical reading of the manuscript. This work was partially supported by Grant-in-Aid for Young Scientists (A) from the Ministry of Education, Science, Sports, and Culture, Japan.

Supporting Online Material

www.sciencemag.org/cgi/content/full/329/5987/93/DC1
Materials and Methods
Figs. S1 to s16
References

2 March 2010; accepted 12 May 2010
10.1126/science.1188995

Generation of genetically modified rats from embryonic stem cells

Masaki Kawamata and Takahiro Ochiya[1]

Section for Studies on Metastasis, National Cancer Center Research Institute, 1-1 Tsukiji, 5-chome, Chuo-ku, Tokyo 104-0045, Japan

Communicated by Takashi Sugimura, National Cancer Center, Tokyo, Japan, June 30, 2010 (received for review April 22, 2010)

At present, genetically modified rats have not been generated from ES cells because stable ES cells and a suitable injection method are not available. To monitor the pluripotency of rat ES cells, we generated *Oct4*-Venus transgenic (Tg) rats via a conventional method, in which Venus is expressed by the *Oct4* promoter/enhancer. This monitoring system enabled us to define a significant condition of culture to establish authentic rat ES cells based on a combination of 20% FBS and cell signaling inhibitors for Rho-associated kinase, mitogen-activated protein kinase, TGF-β, and glycogen synthase kinase-3. The rat ES cells expressed ES cell markers such as *Oct4*, *Nanog*, *Sox2*, and *Rex1* and retained a normal karyotype. Embryoid bodies and teratomas were also produced from the rat ES cells. All six ES cell lines derived from three different rat strains successfully achieved germline transmission, which strongly depended on the presence of the inhibitors during the injection process. Most importantly, high-quality Tg rats possessing a correct transgene expression pattern were successfully generated via the selection of gene-manipulated ES cell clones through germline transmission. Our rat ES cells should be sufficiently able to receive gene targeting as well as Tg manipulation, thus providing valuable animal models for the study of human diseases.

genetic engineering | rat | embryonic stem cells

The laboratory rat was the earliest mammalian species domesticated for scientific research and has been used as an animal model in physiology, toxicology, nutrition, behavior, immunology, and neoplasia for over 150 y (1). Despite this history, rats lag far behind mice in functional genetic studies and the generation of knockout animal models reflecting human diseases because of the absence of germline-competent rat ES cells, which are vital in a reverse genetics approach (2, 3). Recently, gene-targeting rats were created by the zinc finger nuclease strategy (4). However, the system is not available for most researchers because a special technique is required to make algorithm-based sequence-specific DNA nucleases. Thus, establishment of rat ES cells has been desired to produce gene-targeting rats, such as mutant mice, routinely.

Although we established rat ES cell lines with chimeric contribution, none could complete germline transmission (5). Soon after our report, other groups succeeded in establishing rat ES cells with germline transmission by using 2i, mitogen-activated protein kinase (MEK) inhibitor PD0325901, and glycogen synthase kinase-3 (GSK3) inhibitor CHIR99021 (6, 7). The 2i is widely used in the establishment of ES cells or induced pluripotent stem (iPS) cells in mice (8, 9), rats (6, 7, 10), and humans (10). Thus, the inhibition of MEK and GSK3 has been thought to maintain a ground state of pluripotency in various species. Rat iPS cells with chimeric contribution were established by using an inhibitor of type 1 TGF-β receptor Alk5 (A-83-01) with the 2i, although germline transmission was not accomplished (10). Furthermore, a combination of MEK and ALK5 inhibitors dramatically improved the efficiency of iPS cell generation from human fibroblasts (11). These reports indicate that the inhibition of TGF-β signaling also plays a key role in pluripotency.

It is known that rat ES cells present critical problems in that undifferentiated cells cannot proliferate from single cells after enzymatic dissociation (5) and that chromosomal instability is caused by long-term culture, resulting in the failure of germline transmission (5–7). Recently, Watanabe et al. found that a Rho-associated kinase inhibitor Y-27632 (12) blocks apoptosis and enhances the proliferation of human ES cells after their dissociation into single cells by enzymatic treatment (13). The propagated ES cells cultured by Y-27632 were positive for alkaline phosphatase (ALP) and marker genes such as E-cadherin, Oct4, and SSEA4, and the number of chromosomes was normally maintained during long-term culture (13). These recent reports indicate the suitability of cell signaling inhibitors in the establishment of rat ES cells.

To generate genetically modified rats, highly potent ES cells that can stably contribute to germline chimeras have to be established. As a first step, we generated *Oct4*-Venus transgenic (Tg) rats, in which Venus [YFP mutant (14)] is expressed by the *Oct4* promoter/enhancer. This Tg line enables us to monitor the pluripotency of rat ES cells during the process of establishment. We addressed suitable combinations of the signaling inhibitors based on a culture medium that included 20% FBS. As a result, the use of a combination of four inhibitors, Y-27632, PD0325901, A-83-01, and CHIR99021 (termed YPAC), allowed the establishment of authentic rat ES cells and appeared necessary in the blastocyst injection process for the generation of germline chimeras. Finally, we report that high-quality Tg rats retaining reproductive ability can be generated from rat ES cells.

Results

YPAC Maintains Pluripotency in the Outgrowths of *Oct4*-Venus Tg Blastocysts. We first generated a Tg rat carrying an *Oct4*-Venus fluorescence reporter to monitor pluripotency during establishment of rat ES cells and to investigate development of the ES cells into germ cells in fetal gonads of chimeras. The 3.9-kb *Oct4* (also known as *Pou5f1*) promoter includes both the proximal enhancer and distal enhancer, which gives *Oct4* expression in morula, inner cell mass (ICM), epiblast, primordial germ cells (PGCs), and ES cells (15). In the Tg embryo, Venus was detected specifically in PGCs in the gonad (Fig. S1). This result corresponds to previous reports regarding *Oct4*-reporter Tg mice (16).

Outgrowths were examined from the Tg blastocysts in a basic medium containing 20% FBS, which is generally used for mouse ES cell culture, with or without YPAC. In its absence, Venus fluorescence was decreased at day 3 after plating and disappeared at day 7 despite the fact that ES-like cells propagated and formed a domed structure similar to the mouse ES cell colony (Fig. 1*A*). In the presence of YPAC, ICM cells rapidly propagated while maintaining Venus fluorescence even at day 7. The fluorescence was not observed in differentiated cells (Fig. 1*B*). The expression levels of ES cell marker genes *Oct4*, *Nanog*, *Sox2*, and *Rex1* in ICM cells with YPAC were higher than those without YPAC (Fig. 1*C*).

Author contributions: M.K. and T.O. designed research; M.K. performed research; M.K. analyzed data; and M.K. and T.O. wrote the paper.

The authors declare no conflict of interest.

Freely available online through the PNAS open access option.

[1]To whom correspondence should be addressed. E-mail: tochiya@ncc.go.jp.

This article contains supporting information online at www.pnas.org/lookup/suppl/doi:10.1073/pnas.1009582107/-/DCSupplemental.

DEVELOPMENTAL BIOLOGY

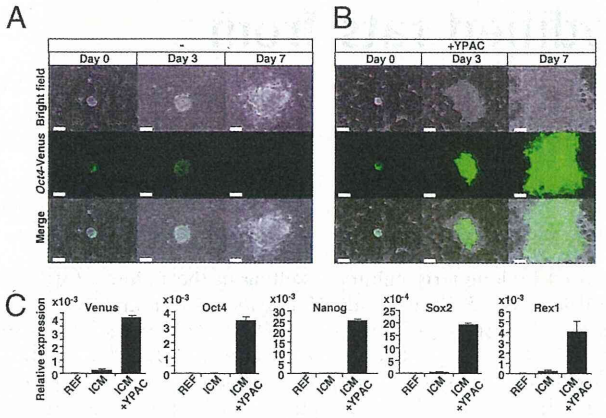

Fig. 1. Outgrowth of ICM cells in YPAC medium. Outgrowth of blastocysts in –YPAC (*A*) or +YPAC (*B*) medium. E4.5 blastocysts were plated onto mitotically inactivated MEFs. (*C*) qPCR analysis of Venus, *Oct4*, *Nanog*, *Sox2*, and *Rex1* in ICM cells. Seven days after plating, RNAs were extracted from domed segments of ICM cells derived from seven or four blastocysts in –YPAC or +YPAC medium, respectively. Transcript levels were normalized to *Gapdh* levels. Data are the mean ± SD of one biological sample assayed in three independent experiments and represent relative expression levels of indicated genes in REFs, ICM (–YPAC), and ICM (+YPAC). (Scale bars: 100 μm.)

In its absence, the decrease of *Oct4* mRNA was parallel to that of Venus mRNA and fluorescence. In the YPAC condition, blastocyst outgrowth was observed in 51 samples for all the tested embryos regardless of the strains (Table 1). The blastocyst strains were derived from a hybrid of Tg Wistar and wild-type Wistar (TgWW, albino), wild-type Wistar (WW, albino), Long–Evans agouti [LEA (LL, agouti)], or a hybrid of Tg Wistar and LEA (TgWL, agouti).

Small Molecules Enable Efficient Derivation and Maintenance of Rat ES Cells. The outgrowths were dissociated into small pieces and replated in the same mouse embryonic fibroblasts (MEFs)/YPAC condition. After undifferentiated colonies appeared, they were split into single cells by Accutase (Innovative Cell Technologies, Inc.). These cells attached on the MEFs and formed domed colonies, which can be passaged continuously (Fig. 2*A Upper Left*). Although most of the ES cells showed ALP activity (Fig. 2*B Left*) and Oct4 protein expression (Fig. 2*D Left*) even after long passages, Venus fluorescence became weak or negative (Fig. 2*A Lower Left*). The expression pattern of Venus mRNA was not parallel to that of *Oct4* between TgWL1 and TgWW1 cell lines (Fig. 2*C*). These results suggest that the function of the *Oct4*-Venus transgene is unavailable in rat ES cell lines. The long-passaged rat ES cells might receive epigenetic silencing effects.

The ES cell lines maintained higher mRNA levels of ES cell marker genes *Oct4*, *Sox2*, *Nanog*, and *Rex1* compared with rat embryonic fibroblasts (REFs) (Fig. 2*C*). Microarray analyses also indicated that global gene expression was remarkably different between ES cells and REFs but similar between the three ES cell lines TgWL1, TgWW1, and LL1 (Fig. S2). Nanog and Sox2 proteins were also detected in ES cells (Fig. 2*D*). The karyotypes of 50 cells were analyzed by G-band staining. Most of the cells exhibited a normal chromosomal number of 42 in TgWL1 (70%, XX, P14), TgWL2 (84%, XX, P7; Fig. 2*E*), TgWW1 (92%, XX, P5), and LL1 (84%, XX, P6). TgWW1 cells (2.6×10^6) could form a teratoma 34 d after transplantation under the skin of an immunodeficient SCID mouse. A histological examination showed that the tumor contained all three germ layers, including the intestinal epithelium (endoderm), cartilage (mesoderm), and neuronal rosette (ectoderm) (Fig. 2*F*).

Table 1. Establishment of rat ES cells from blastocysts in YPAC medium

Strain	No. ICMs	Outgrowth†	Continue	Cell line‡
TgWL	2	2	2	2
TgWW	15	15	1	1
WW	9	9	1	1
LL	19	19	2	2
TgWW*	3	3	2	2
WW*	3	3	0	0
Total	51	51 (100%)	8	8 (100%)

*Specific serum was used (FBS for MEF culture; EQUITECH-BIO, Inc.).
†Outgrowth refers to the expansion of the ICM.
‡Cell line refers to continuous culture of at least seven passages. Single-cell passage was begun at passages 1–3. Domed colonies with undifferentiated cells are continuously formed from single cells.

To confirm the effect of Y, the rat ES cells were cultured in a PAC medium. Under this condition, sparse colonies appeared because of a failure in the adherence process of single cells on MEFs, although the colonies kept undifferentiated morphology and ALP activity (Fig. 2*A Middle* and *B Middle*). Although only Y enabled most of the single cells to adhere on MEFs and to proliferate, they were differentiated and did not show ALP activity (Fig. 2*A Right* and *B Right*).

The classic method to induce ES cell differentiation is to allow the cells to grow in suspension and to form 3D aggregates known as embryoid bodies (EBs) (17). Dissociated ES cells were plated into low-cell-binding dishes in the basal medium. EBs could be formed from the ES cells at a much lower efficiency compared with their formation from mouse ES cells (Fig. 2*E*). The expression of marker genes was decreased during the process of EB differentiation (Fig. 2*I*). In the presence of PAC, cells aggregated with high efficiency and formed a clear 3D structure (Fig. 2*F*). The EBs with PAC at day 7 still sustained high expression levels of the marker genes (Fig. 2*I*). These results suggest that PAC enables ES cells to maintain pluripotency, whereas for rat ES cells to adhere on MEFs, Y is necessary.

YPAC Injection Engenders Germline Chimeras. First, we produced stable transfectant ES cells expressing cyan fluorescence from a CAG-AmCyan1 transgene to monitor cell fate in the blastocyst after injection or chimerism in fetuses (Fig. 3*A*). Before generation of the chimera, the potential of YPAC was investigated during the injection and blastocyst incubation processes because the rat ES cells tended to differentiate easily in the absence of inhibitors (Fig. 2 *A*, *B*, and *E*). There was no difference between normal and YPAC injection 5 h after incubation; in both cases, several cyan-positive cells adhered on the ICM and trophectoderm. However, 30 h after incubation, few cyan-positive cells existed in the blastocysts in the absence of YPAC, whereas in its presence, several cells remained on the ICM surface. Furthermore, blastocyst shape was maintained by the addition of YPAC even after incubation for 30 h (Fig. 3*B*). This result suggests that administration of YPAC during the injection process causes both ES cells and recipient blastocysts to block differentiation or apoptosis. This YPAC injection method enabled generation of chimeric embryos showing positivity for cyan but negativity for Venus in the surface of skin and kidney. Venus-positive cells were detected specifically in the gonads, showing the successful development of the ES cells into germ cells (Fig. 3*C*). We also succeeded in generating germline chimeras using all other cell lines by detecting Venus fluorescence in the fetal gonad (Table 2). The germline chimeras were detected in 2 of 12 fetuses by using long-cultured TgWL2 cells at passage 22 (Table 2 and Fig. S3).

To investigate the pluripotent ability of ES cells, we carried out a single-cell injection into a blastocyst. After injection of the

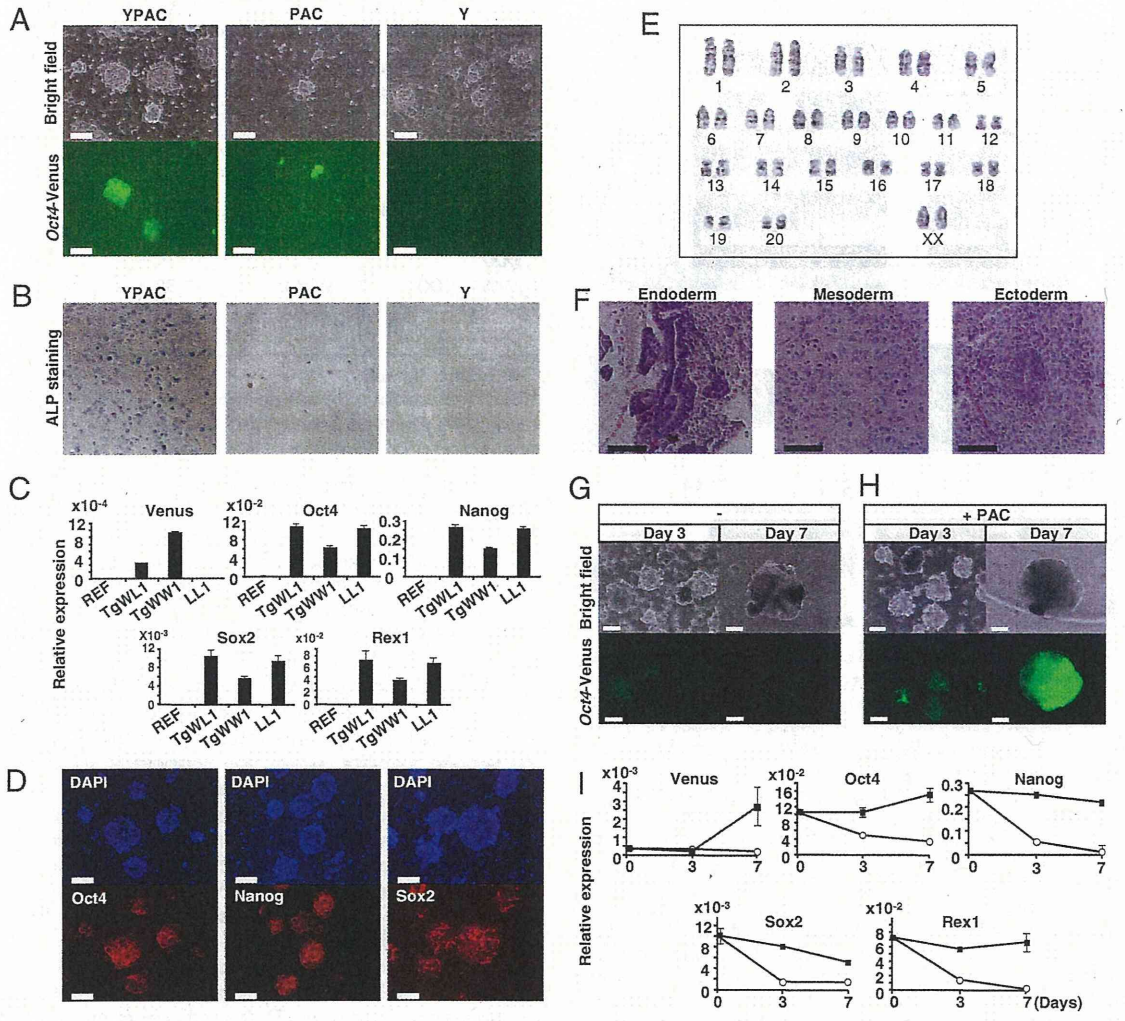

Fig. 2. Characterization of rat ES cells. Effect of Y-27632 (*A*) and ALP (*B*) staining. Dissociated single cells (1×10^5 TgWW1, passage 6) were plated into a well of six-well plates under the condition of MEFs with YPAC (*Left*), PCA (*Center*), or Y (*Right*). (*B*) ALP staining in these cells. (*C*) qPCR analysis of Venus, *Oct4*, *Nanog*, *Sox2*, and *Rex1* in rat ES cell lines. Transcript levels were normalized to *Gapdh* levels. Data are the mean ± SD of one biological sample assayed in three independent experiments and represent the relative expression levels of indicated genes in REF, TgWL1, TgWW1, and LL1. (*D*) Immunofluorescence staining for *Oct4*, *Nanog*, and *Sox2* in rat ES cells. (*E*) Cytogenetic analysis in rat ES cells by G-band staining. Representative data of TgWL2 at passage 7 indicate a chromosomal number of 42, including an XX gender chromosome. (*F*) Histological sections of a teratoma derived from a TgWW1 ES cell line showing three germ layers. Embryoid bodies (TgWL1) were produced in a basic ES cell medium with (*H*) or without (*G*) three PAC inhibitors, excluding Y-27632. A time-course experiment was performed, and the EBs were observed at days 3 and 7. (*I*) qPCR analysis of Venus, *Oct4*, *Nanog*, *Sox2*, and *Rex1* in EBs. Transcript levels were normalized to *Gapdh* levels. Data are the mean ± SD of one biological sample assayed in three independent experiments and represent the relative expression levels of indicated genes in EBs produced without inhibitors (○) or with PAC (■) at days 0, 3, and 7. (Scale bars: 100 μm.)

TgWW1 cell at passage 9, the single cell attached to the internal surface of the blastocyst (Fig. 3*D*). In an embryo day (E) 16.0 fetus gonad, germ cell differentiation was confirmed by the detection of Venus fluorescence (Fig. 3*E*).

To generate coat-color chimeras, TgWL1 cells were injected into Wistar blastocysts using the YPAC injection method. Eight of 23 coat-color chimeras were obtained from the TgWL1 cell line at passage 11 or 12 (Fig. 3*F Right* and Table 3). Without the YPAC injection method, a coat-color chimera was hardly generated despite the fact that the same cell line, TgWL1, was used at earlier passages 6–8 (Fig. 3*F Left* and Table 3). Only 1 male chimera of 44 pups was obtained, but the chimerism was very sparse (Fig. S4). The generation of coat-color chimeras was successful in all six cell lines (Table 3). Those from cell line TgWW1 or LL1 are shown in Fig. S5. After mating with male rats, germline transmission was accomplished in adult female chimeras derived from all six cell lines independent of rat strains (Fig. 3*G* and Table 3). Genotyping analysis indicated that the *Oct4*-Venus transgene of the ES cells (TgWL2) was transmitted to filial (F)1 germline offspring with an agouti coat color (Fig. 3*H*).

Generation of ES Cell-Derived Tg Rats. We proposed to generate ES cell-derived transgenic (esTg) rats harboring the *Oct4*-Venus transgene, which shows a correct Venus expression pattern similar to Oct4 protein (Fig. 2*D*). After introduction of the *Oct4*-Venus transgene containing the same *Oct4* promoter/enhancer region as used in the generation of the conventional transgenic (cvTg) rats, 15 Venus-positive colonies (LL2 line) were picked up. After two passages, silencing of Venus gene expression occurred in 13 of 15 clones, resulting in an apparent heterogeneity in the fluorescence of Venus-positive clones (Fig. 4*A*, arrowheads), whereas only 2 clones kept homogenous Venus fluorescence (Fig. 4*B*). Chimeric

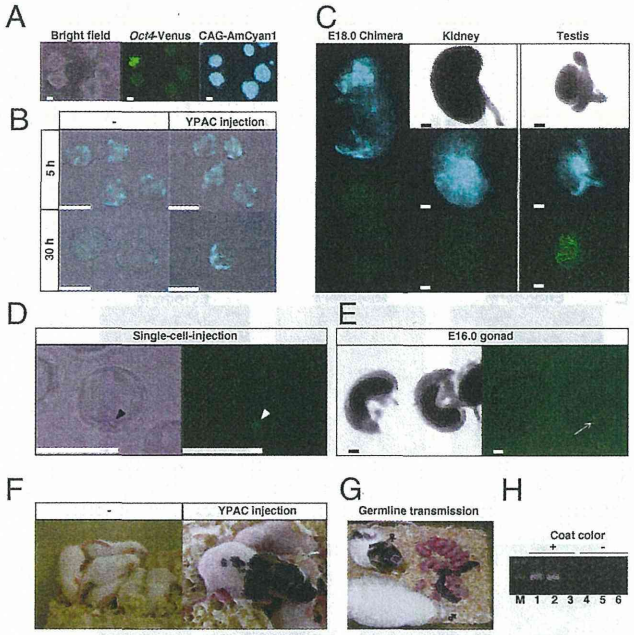

Fig. 3. Generation of germline chimeras by YPAC injection method. (*A*) Expression of AmCyan1 in stable transfectant clones (TgWW1 + C) generated by nucleofection with CAG-AmCyan1 plasmids. (*B*) Effect of YPAC during injection process. The basic ES cell medium with (*Right*) or without (*Left*) YPAC was used during the processes: injection of TgWW1 + C cells into blastocysts and incubation of the blastocysts for 30 h. (*C*) Generation of germline chimeras in embryos. TgWW1 + C cells were injected into Wistar blastocysts. Venus or AmCyan1 fluorescence was observed in E18.0 whole embryo, kidney, and testis. (*D* and *E*) Generation of germline chimeras by single-cell injection. (*D*) A single cell (TgWW1) was injected into a blastocyst. The image shows the injected blastocyst 3 h after incubation. The arrowhead indicates the injected single cell. (*E*) Venus-positive germ cells were detected in gonad at E16.0 (arrow). (*F*) Generation of coat-color chimeras by the YPAC injection. (*G*) Germline transmission in adult chimeras. The chimera (TgWL1) was mated with a Wistar male rat. Germline pups (4 of 16) were confirmed by an agouti coat color. (*H*) Genotyping analysis of F1 offspring of female chimera (TgWL2). The Venus region was amplified by PCR from genomic DNA of tail. M, 100-bp DNA marker; 1, 2, and 3, germline offspring with an agouti coat color; 4, 5, and 6, coat color-negative (albino) offspring. (Scale bars, *A*, *B*, and *D*: 100 μm; *C* and *E*: 300 μm.)

rats were produced via injection of the stable clone into Wistar blastocysts. Furthermore, germline transmission with the *Oct4*-Venus transgene was accomplished in the female chimeras (Fig. 4*C* and Table 3). The esTg embryos at 16.0 days postcoitum (dpc) exhibited Venus fluorescence in the gonads (Fig. 4*D*). The esTg rats were able to mature to adults without apparent abnormalities and had normal reproductive ability. We established ES cell lines from esTg blastocysts to confirm an expression pattern of Venus fluorescence. During outgrowth, their Venus expression pattern (Fig. 4*E*) was similar to that of cvTg blastocysts (Fig. 1*B*). However, long-passaged esTg cell lines ($n = 3$) maintained stable Venus expression in the ES cells (Fig. 4*F*). This result indicates our success in generating high-quality esTg rats possessing a correct expression pattern of Venus under the *Oct4* promoter/enhancer.

Discussion

Our results demonstrated that the use of a combination of serum and cell signaling inhibitors during outgrowth, cell culture, and blastocyst injection leads to the generation of germline chimeras with extremely high efficiency. Furthermore, we generated genetically modified rats from ES cells, termed esTg rats, growing up healthily and retaining reproductive ability. The advantage of this technology of using rat ES cells is that we can select Tg ES

Table 2. Summary of germline chimeras: Germ cell development in fetal gonad judged by Venus fluorescence

Cell line (gender)	Passage no.	Host blastocyst	Injected embryos	Fetal no.	Germline chimera
TgWL2 (XX)	6	LEA	43	9	1M1F
	22	Wistar	13	3	1F
		Wistar/LEA	23	9	1F
TgWW1 (XX)	6, 7	Wistar	53	9	2M7F
TgWW1 + C (XX)	8	Wistar	46	9	1M1M or F
TgWW1s (XX)	9	Wistar	35	8	1F
TgWW2* (XX)	8	Wistar	28	1	1M

F, female; M, male.
*ES cell line established by using specific serum. TgWW1 + C refers to a stable transfectant possessing CAG-AmCyan1 transgene.

cell clones that possess a correct gene expression pattern of the transgene. Our *Oct4*-Venus esTg rats will be useful for the generation of iPS cells as a pluripotency monitoring system with respect to previous work in mice (9, 18, 19). For further study, addressing the mechanism of the silencing effect on the transgenes should be crucial.

The complete generation of esTg rats might be based on the use of a culture medium containing 20% serum and YPAC, which might provide strong protectection from cell damage during gene introduction with electrical stimuli and maintain pluripotency with a stable karyotype during the cloning and expansion process. To support viability, serum was temporally used in a previous report when rat ES cells were electroporated and cultured overnight in a 2i medium (6). Such efforts are not necessary with our rat ES cells, which are tolerant to the damage induced by gene introduction because of the presence of 20% serum in the YPAC medium. Furthermore, we have confirmed that drug selection through the use of G418 is efficient in rat ES cells for generating genetically modified rats.

Previous work has suggested that the failure in the establishment of authentic rat ES cells over the past 2 decades was attributable to the presence of serum (6, 7). Indeed, serum may contain various kinds of nutrient factors as well as differentiation factors for rat ES cells (20). The reason why we succeeded in the establishment of such significant pluripotent cell lines might be attributable not only to the signaling inhibitors shielding ES cells from differentiation but to the use of the nutrients in the serum. Monitoring serum quality for better ES cell culturing is extremely important. Nevertheless, our combination of YPAC and different serum, which is used for culturing MEFs, allowed stable establishment of rat ES cell lines. Our success is thus partly attributable to the strong potential of YPAC in the maintenance of ES cells regardless of differentiation factors under different culture conditions.

It is noteworthy that leukemia inhibitory factor (LIF) was not necessary in our culture medium, although recent reports have suggested that its addition improved rat ES or rat iPS cell ability to suppress differentiation (6, 7, 10). It has been shown that LIF is the key cytokine secreted by feeders in supporting mouse ES cell self-renewal (21, 22) and that LIF was able to replace the requirement for feeders in propagation (23, 24). Ying et al. (8) demonstrated that a combination of PD0325901 and CHIR99021 enabled mouse ES cells to maintain pluripotency by substituting LIF, feeders, and serum. Considering these reports, the addition of LIF in our culture condition might be dispensable because of the inclusion of serum, MEFs, and the two inhibitors. Actually, the expression level of *Tbx3,* which is involved in mediating LIF signaling (25), was up-regulated in the rat ES cells. Moreover, we found that the expression of a suppressor of cytokine signaling 3 (*SOCS3*), which is one of the STAT3's direct target genes (26),

Table 3. Summary of germline chimeras: Chimeras and germline transmission judged by coat color of F1 pups

Cell line (gender)	Passage no.	Host blastocyst	Injected embryos	Pup no.	Chimera no.	Mating no.	Germline chimera
−YPAC injection							
TgWL1 (XX)	6–8	Wistar	226	44	1M*	0	—
+YPAC injection							
TgWL1 (XX)	11, 12	Wistar	123	23	3M5F	1M3F	1F
TgWL2 (XX)	4, 6	Wistar	70	10	2M3F	1M3F	2F
TgWW1 (XX)	9	Wistar/ LEA	79	19	5M3F	3F	1F
WW1 (XX)	10	LEA	27	7	2M1F	1F	1F
LL1 (XX)	4, 6	Wistar	107	13	3F	2F	1F
LL2 (XX)	9	Wistar	52	6	3F	3F	2F

F, female; M, male.
*Coat-color contribution is sparse (Fig. S5).

was up-regulated after stimulation with rat LIF (27) even in the YPAC medium. Thus, it seems possible to improve the culture condition further by the administration of rat LIF.

The six established ES cell lines in this work were all female. This result does not correspond to mice, because most of the mouse ES cell lines are male. In our present study, we continued to culture rat ES cell lines exhibiting rapid cell proliferation, resulting in the establishment of six female lines. Thus, we speculate that female blastocysts are suitable for the establishment of rat ES cells or that the addition of MEK and GSK3 inhibitors to the culture medium facilitates female-specific rapid cell growth in rat ES cells. A previous study using MEK and GSK3 inhibitors also reported that six of seven rat ES cell lines were female (6).

Although two groups reported the establishment of authentic rat ES cells, only one of several cell lines accomplished germline transmission in each group (6, 7). So far, there is no report of successful generation of knockout/knockin rats from ES cells. Thus, trials to produce more potent cell lines and to find the optimal combination of rat strains for donor ES cells, host blastocysts, and recipient foster female animals remain to be addressed (6, 7). In this study, our YPAC culture and injection method overcame the difficulty of completing germline transmission in all six ES cell lines independent of rat strains. The YPAC condition will enable the selection of preferable rat strains for the generation of genetically modified rats from ES cells, bringing great advantages to research for strain-specific disease models. We believe that the availability of our rat ES cells and the YPAC injection technique will also open up a valuable platform for routinely generating knockout/knockin rats, holding out the promise for generation of previously undescribed disease models.

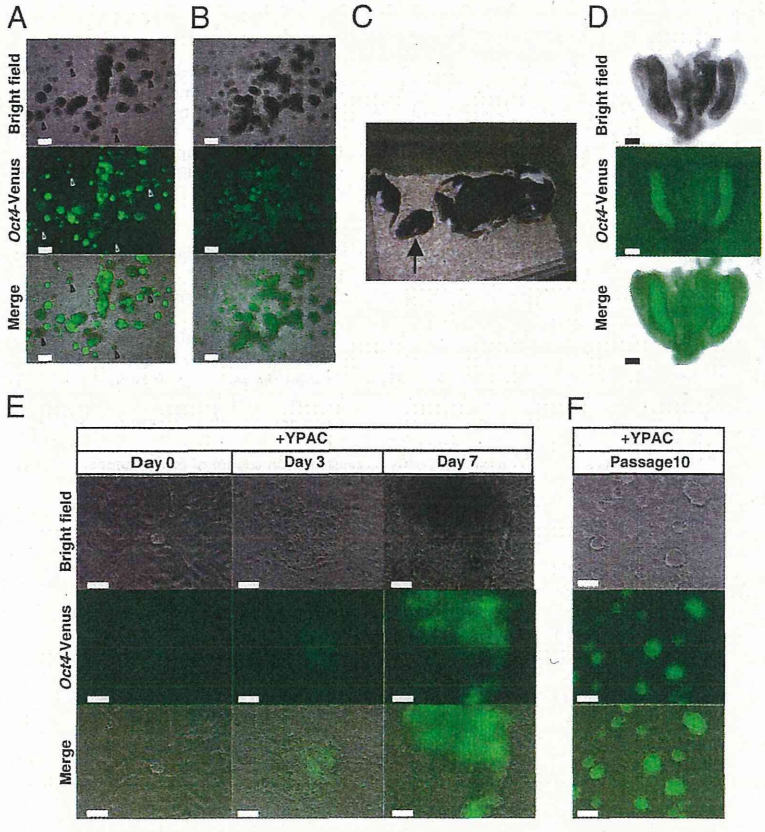

Fig. 4. Generation of Tg rats from ES cells. (*A* and *B*) Cloning and expansion of *Oct4*-Venus transfectants. An *Oct4*-Venus transgene was introduced into ES cells (LL2) at passage 5. Venus-positive clones were passaged without drug selection. (*A*) Arrowheads indicate ES cells with Venus expression silenced. (*B*) ES cells with homogeneous expression of *Oct4*-Venus. (*C*) Generation of Tg rats from ES cell clone displaying homogeneous expression of *Oct4*-Venus. An arrow indicates esTg rats through germline transmission from the chimeric rat. (*D*) Venus fluorescence in gonads of an esTg embryo at 16.0 days postcoitum (dpc). (*E*) Outgrowth of esTg blastocyst in YPAC medium. (*F*) Rat ES cell line derived from an esTg blastocyst. The expression of *Oct4*-Venus did not receive a silencing effect even after 10 passages. (Scale bars, *A*, *B*, and *D*: 300 μm; *E* and *F*: 100 μm.)

DEVELOPMENTAL BIOLOGY